Soft salts based on platinum(II) complexes with high emission quantum efficiencies in the near infrared region for *in vivo* imaging

Jun Li,[‡b] Yun Ma,[‡a,c] Suyi Liu,[c] Zhu Mao,[e] Zhenguo Chi,[e] Peng-Cheng Qian*[f] and Wai-Yeung Wong*[a,b,d]

Two soft salts (S1 and S2) based on platinum(II) complexes with a near-infrared emission have been designed and synthesized. It has been demonstrated that S2 has a high photostability and a low cytotoxicity, and it has been successfully applied to *in vivo* imaging for the first time.

In recent years, near-infrared (NIR) materials have shown emerging and promising applications in OLEDs,[1] night-vision technology,[2] and photodynamic therapy.[3] In particular, luminescent probes emitting in the NIR region with a high quantum efficiency are essential for *in vivo* imaging due to their deep tissue penetration, low photo-damage, and minimal background fluorescence.[4] The most popular NIR imaging agents are quantum dots (QDs)[5] and organic dyes.[6] However, QDs are often cytotoxic because heavy metal ions are released in an oxidative environment. Most NIR organic dyes have small Stokes shifts and poor photostabilities, which are not suitable for *in vivo* imaging. Consequently, the development of alternative NIR luminescent probes with a high quantum efficiency, a large Stokes shift, and a low cytotoxicity remains a challenge. Phosphorescent transition metal complexes (TMCs) have high quantum efficiency, high photostability, easy tunability of the emission wavelength, and remarkably large Stokes shift.[3a,7] This makes them potential candidates for *in vivo* imaging applications. Despite the advantages of phosphorescent TMCs-based probes, the emission wavelength of most of the previously reported probes is located in the visible spectrum. Therefore, NIR probes based on phosphorescent TMCs still need to be further developed.

Soft salt complexes are emerging phosphorescent materials that consist of two photoactive organometallic complexes with opposite charges linked by an electrostatic attraction and van der Waals forces.[8] Such materials can comprise of different metal complexes, and consequently have both interesting structural and photophysical properties. Although the research on phosphorescent soft salt complexes is still in its infancy, these materials have a great potential in various optoelectronic areas. For example, many soft salts based on iridium(III) complexes have been prepared for different applications in organic light-emitting diodes,[9] electrochromic switches,[10] bioimaging,[11] and porous crystals.[12] In addition, Yam *et al.* have reported a series of water-soluble platinum(II)bzimpy complex salts (bzimpy = 2,6-bis (benzimidazol-2′-yl)pyridine) that form infinite 1-D chains through Pt···Pt and π-π stacking interactions.[13] These supramolecular nanostructures have a bright NIR emission. The high efficiency is attributed to the metal-metal-to-ligand charge transfer (MMLCT) induced by the very close Pt···Pt interaction (~3.4 Å). This is an effective method to obtain NIR PTMCs, which has been verified by several previous studies.[14]

In this work, we have designed and prepared soft salts based on two platinum(II) complexes with a bright NIR emission. The platinum(II) complexes of (Pt-dfppy)$^-$NBu$_4^+$ (**A1**, dfppy = 2-(2,4-difluorophenyl)pyridine) and (Pt-piq)$^-$NBu$_4^+$ (**A2**, piq = 1-phenylisoquinoline) were chosen as the anionic components. The

[a] *Department of Applied Biology and Chemical Technology, The Hong Kong Polytechnic University, Hung Hom, Hong Kong, P. R. China. E-mail: wai-yeung.wong@polyu.edu.hk*

[b] *Department of Chemistry, Hong Kong Baptist University, Waterloo Road, Hong Kong, P. R. China*

[c] *Key Laboratory for Organic Electronics and Information Displays (KLOEID) and Institute of Advanced Materials (IAM), Nanjing University of Posts and Telecommunications (NUPT), 9 Wenyuan Road, Nanjing 210023, Jiangsu, P. R. China.*

[d] *The Hong Kong Polytechnic University Shenzhen Research Institute Shenzhen, P. R. China.*

[e] *PCFM Lab, GD HPPC Lab, Guangdong Engineering Technology Research Center for High- performance Organic and Polymer Photoelectric Functional Films, State Key Laboratory of Optoelectronic Material and Technologies, School of Chemistry, Sun Yat-Sen University, Guangzhou 510275, P. R. China*.

[f] *Key Laboratory of Environmental Functional Materials Technology and Application of Wenzhou City, Institute of New Materials & Industry, College of Chemistry & Materials Engineering, Wenzhou University, Wenzhou 325035, P. R. China.*

[‡] These authors contributed equally to this work.

platinum(II) complexes of $[Pt(tpp)(ed)]^{+}Cl^{-}$ (**C1**, tpp = 2-(thiophen-2-yl)pyridine, ed = ethylenediamine) and $[Pt(dfppy)(ed)]^{+}Cl^{-}$ (**C2**) were selected as the cationic components. The soft salt complexes were formed by these two oppositely-charged components *via*

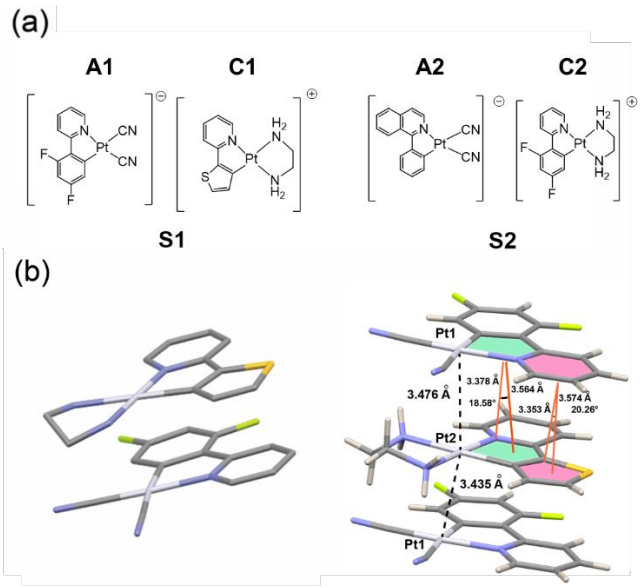

Fig. 1 (a) Chemical structures of soft salt complexes **S1** and **S2**. (b) Single crystal of **S1** (CCDC1967647) and its perpendicular view illustrating the alternation of Pt complex cations and anions.

electrostatic interactions. In addition, these complexes have square-planar geometry, which facilitates very close Pt···Pt and π···π interactions, resulting in a NIR emission in the solid state. Furthermore, the synthesized NIR soft salt complex **S2** has a low cytotoxicity and a good photostability that allowed its use for *in vivo* imaging.

The anionic and cationic platinum(II) complexes were synthesized according to the literature methods.[15] The platinum(II) soft salts were prepared through the simple metathesis reactions of anionic platinum(II) complexes and 1.1 equivalents of cationic platinum(II) complexes in solution. The detailed synthetic procedures are provided in the electronic supplementary information. The desired soft salt complexes were characterized by ^{1}H NMR, ^{13}C NMR (Figs. S1-S6), MALDI-TOF MS spectrometry, and X-ray crystal structure analysis.

Single crystals of the **C1** and soft salt complex **S1** were obtained by slow evaporation of its ethanol solution. The packing diagram of **C1** displayed that the distance between two adjacent Pt atoms is 4.336 Å (Fig. S7), suggesting the absence of Pt···Pt interaction in **C1**. Compared to it, the X-ray crystal structure of **S1** showed that the **C1** cations are placed between adjacent **A1** anions, forming alternating layers of two oppositely-charged ions (Fig. 1b). Moreover, the single crystals of **S1** presents a distance between two adjacent Pt atoms of 3.467 Å, clearly indicating the presence of a Pt···Pt interaction. The plane of the dfppy (from **A1**) and the 2-(thiophen-2-yl)pyridine plane (from **C1**) are almost parallel since the angle between both planes is only 0.662° and the distance between both planes is 3.564 Å. This suggests the existence of a strong π-π stacking. The intramolecular Pt···Pt and π-π interactions likely resulted in the large bathochromic shift in the solid-state emission of the soft salt complexes **S1** and **S2**. Some selected parameters of the single crystal are summarized in Tables S1 and S2.

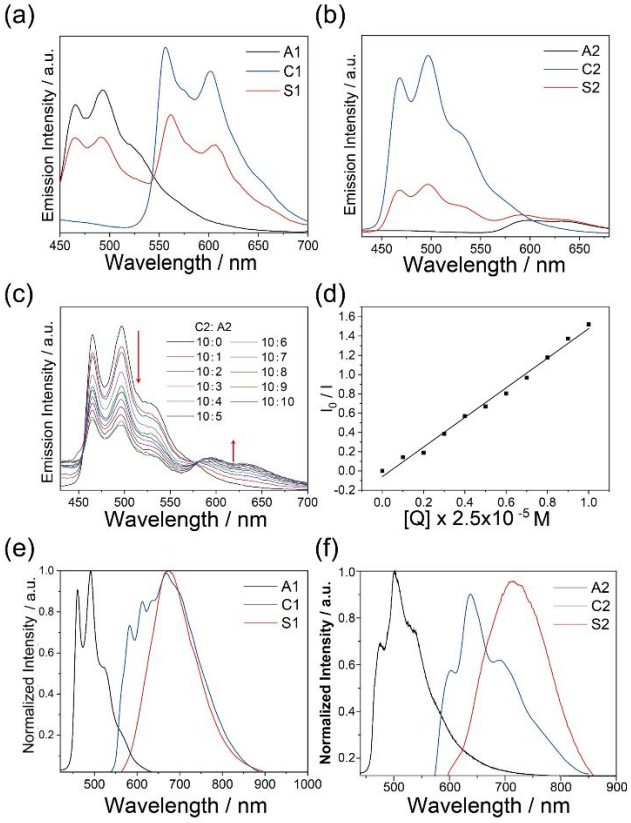

Fig. 2 (a) PL spectra of **A1**, **C1** and **S1** in MeOH (1×10^{-4} M). (b) PL spectra of **A2**, **C2** and **S2** in MeOH (1×10^{-4} M). (c) PL spectra of cationic complex **C2** (10^{-5} M) in MeOH solution with various amounts of anionic complex **A2**. (d) Stern–Volmer plot of the quenching study between **C2** and **A2** ([Q] = [**A2**]), R^2=0.99. (e) PL spectra of **A1**, **C1** and **S1** in the solid state (f) PL spectra of **A2**, **C2** and **S2** in the solid state.

The photophysical properties of the synthesized cationic complexes, the anionic complexes, and the soft salt complexes were investigated. Their UV/visible absorption spectra were recorded in methanol at room temperature (Fig. S8). All complexes showed multiple absorption bands. The intense absorption bands below 350 nm are attributed to the spin-allowed ligand-centered transition (^{1}LC). The moderately intense absorption bands within 350-400 nm are attributed to the singlet metal-to-ligand charge-transfer transition ($^{1}MLCT$) and the weak bands above 400 nm are assigned to the triplet metal-to-ligand charge-transfer transition ($^{3}MLCT$) and the spin-forbidden ligand-centered transition (^{3}LC). Additionally, all platinum(II) complexes have a weak emission in methanol at room temperature. Their photoluminescence (PL) spectra are shown in Figs. 2a and 2b. The emission wavelength of these complexes can be significantly tuned from 465 to 632 nm depending on the nature of the cyclo-metalating ligands. The emission bands of all complexes show vibronic progressions, which originates from the triplet ligand-centered transition on the cyclometalated ligands.

Fig. 2c shows that the emission intensities of short wavelengths were remarkably quenched in the soft salt complexes. Consequently, we performed a quenching study according to the equation of $I_0/I = 1 + k_q[Q]$, where I_0 and I indicate the PL intensity of **C2** with and without the quencher **A2**, k_q refers to the

Table. 1 Photophysical properties of **A1**, **C1**, **S1** and **A2**, **C2**, **S2** in the solid state

Name	λ_{em}/ nm	QY / %	Lifetime / μs
A1	460, 492, 524	60	19.0
C1	582, 610, 667	3.3	6.53
S1	674	20.3	2.95
A2	602, 637, 692	2.6	6.83
C2	464, 495, 524	85.1	9.13
S2	718	17.0	0.40

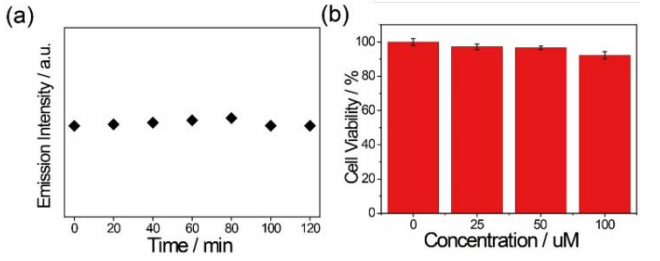

Fig. 3 (a) Emission intensity of a DMSO/PBS (v : v = 1 : 99) mixture of **S2** (1×10^{-4} M) under continuous laser excitation at 405 nm. (b) Cell viability values (%) assessed using a MTT (MTT = 3-(4,5-dimethylthiazol-2-yl)-2,5-diphenyltetrazoliumbromide) proliferation test versus incubation concentration of **S2**.

experimental quenching rate constant, and [Q] represents the molar concentration of the quencher **A2**. The emission intensity of **C2** decreases with the addition of increasing equivalents of **A2**, which is likely due to the intermolecular triplet–triplet energy transfer. The plot shows a very good linear relationship with a coefficient of regression R^2 = 0.99 and the calculation gives a k_q of 5.05×10^9 M^{-1} (Fig. 2d), suggesting the energy transfer/quenching process is efficient in **S2**.[9a]

Next, we studied the PL properties of these platinum(II) complexes in the solid state, as shown in Figs. 2e and 2f. The data are summarized in Table 1. Fig. 2e shows that **A1** had a sharp structured emission band at 460-524 nm in the solid-state with a high quantum yield (QY) of 60.0%. The strong sky-blue colour observed can be assigned to the isolated monomer because the bulky n-Bu_4N^+ cations separate two neighbouring platinum(II) complexes. Similarly, the emission peaks of **A2** (λ_{max} = 637 nm, QY = 2.6%) also came from the platinum(II) monomer. For the cationic components, **C1** had a weak red emission at 667 nm with QY of 3.3 % in the solid state, while **C2** showed strong emission intensity at 495 nm with a QY of 85.1% (Figs. 2e and 2f and Table 1). Both **S1** and **S2** had a bright NIR emission in the solid state with a single peak at 674 and 718 nm and a high QY of 20.3% and 17.0%, respectively (Table S3). This characteristic emission is likely to come from the MMLCT transitions according to previous reports.[1] To demonstrate the important role of the Pt(II) anionic component of the soft salt complex in contributing to the bright NIR emission, cationic complex with different counter anions (Br^-, BF_4^-, and PF_6^-) were prepared and their PL properties were investigated. Fig. S9 showed the PL spectra of these cationic complexes in the solid state, and their emission profiles are quite different from that of **S1**. In addition, the emission quantum yields of these cationic complexes were measured to be 1.6%, 1.8%, and 3.9%, which are much lower than that of **S1**. The molecular packing illustrated in Fig. 1b and Fig. S7 confirmed the difference in the Pt···Pt interactions of these two different complexes.

The morphology of **S2** in DMSO/PBS (v : v = 1 : 99) mixture was characterized by transmission electron microscopy (TEM). As shown in Fig. S10, the image indicates that the nanoparticles were formed, which had a spherical shape with diameters ranging from 40 to 60 nm. Good photostability in aqueous solution is important for biological applications, especially in long-duration studies. Considering that the emission wavelength of **S2** is located in the NIR region, it was selected as a potential probe for *in vivo* imaging. The PL intensity evolution of **S2** was investigated by monitoring the change in emission when dispersed in a dimethylsulfoxide (DMSO)/phosphate buffer solution (PBS) (v : v = 1 : 99) mixture at different irradiation times. Fig. 3a indicates no significant PL intensity decrease after a continuous excitation at 405 nm for 2 h, which is sufficiently long to perform *in vivo* imaging experiments.

To evaluate the cytotoxicity, the viability of HeLa cells was investigated after incubation with **S2** at different concentrations. Fig. 3b shows the cytotoxicity results of **S2** when incubated with HeLa cells for 24 h. The cellular viabilities were over 90% for **S2** at concentrations within 25–100 μM, indicating a low cytotoxicity of this soft salt complex. This confirms it is a good candidate for biological imaging.

To demonstrate the potential application of the soft salt complexes prepared for *in vivo* NIR phosphorescent imaging, **S2** was used to image live mice. Firstly, a DMSO solution of **S2** was rapidly injected into a PBS buffer (v : v = 1 : 99) under continuous ultrasound to form nanoparticles with strong NIR emission (Figs. S11 and S12). Then, the DMSO/PBS solution of **S2** was injected into a small mouse, which had a strong NIR emission under the live fluorescence imaging system, whereas there was no signal in the DMSO/PBS mixture (Fig. 4a). Figs. 4b and 4c show that no luminescent signal was detected with an excitation of 440 nm when the DMSO/PBS solution was injected, whereas an intense emission was observed when a DMSO/PBS (v : v = 1 : 99) mixture of **S2** (1×10^{-4} M, 200 μL) was injected. This suggests that the soft salts based on platinum(II) complexes have a strong potential to be applied as the bright NIR probe for *in vivo* imaging.

In summary, we developed two soft salts based on platinum(II) complexes with a NIR emission at a high quantum efficiency. Their single crystal structures revealed strong Pt···Pt and π-π interactions, which might be responsible for the NIR emission *via* MMLCT transitions. The soft salt complex **S2** has a good photostability and a low cytotoxicity. Hence, **S2** was successfully employed as a NIR probe for *in vivo* imaging in live mice. Overall, our design principle offers a new route to obtain NIR emitters with soft salt complexes, which has a tremendous potential for biological applications.

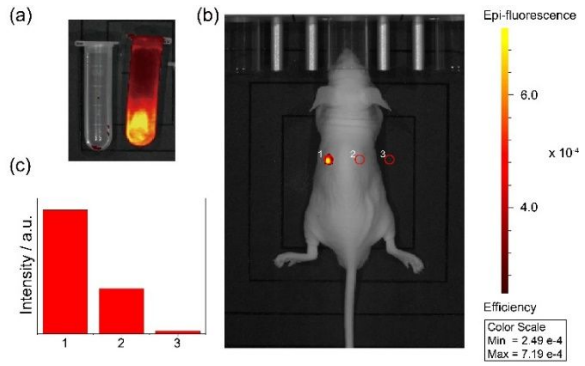

Fig. 4 (a) PL images of the DMSO/PBS mixture and DMSO/PBS **S2** solution. (b) In vivo imaging of mice after subcutaneous injection of DMSO/PBS (v : v = 1 : 99) **S2** solution upon excitation at 440 nm. (c) Emission intensity of different areas in mice and background.

Acknowledgements

The authors are grateful to the financial support from National Natural Science Foundation of China (51873176, 21701087 and 21828102), the Hong Kong Research Grants Council (PolyU 153062/18P and C6009-17G), the Hong Kong Polytechnic University (1-ZE1C and 847S) and the Foundation of Wenzhou Science & Technology Bureau (No. W20170003).

Conflicts of interest

There are no conflicts to declare.

Notes and references

1 (a) K. Tuong Ly, R.-W. Chen-Cheng, H.-W. Lin, Y.-J. Shiau, S.-H. Liu, P.-T. Chou, C.-S. Tsao, Y.-C. Huang and Y. Chi, *Nat. Photonics*, 2017, **11**, 63–68; (b) A. Graf, C. Murawski, Y. Zakharko, J. Zaumseil and M. C. Gather, *Adv. Mater.*, 2018, **30**, 1706711; (c) Y. Yuan, Y. Hu, Y.-X. Zhang, J.-D. Lin, Y.-K. Wang, Z.-Q. Jiang, L.-S. Liao and S.-T. Lee, *Adv. Funct. Mater.*, 2017, **27**, 1700986; (d) S. Wang, X. Yan, Z. Cheng, H. Zhang, Y. Liu and Y. Wang, *Angew. Chem.Int. Ed.*, 2015, **54**, 13068–13072.

2 (a) C. Borek, K. Hanson, P. I. Djurovich, M. E. Thompson, K. Aznavour, R. Bau, Y. Sun, S. R. Forrest, J. Brooks, L. Michalski and J. Brown, *Angew. Chem. Int. Ed.*, 2007, **46**, 1109–1112; (b) E. Song, X. Jiang, Y. Zhou, Z. Lin, S. Ye, Z. Xia and Q. Zhang, *Adv. Opt. Mater.*, 2019, 1901105.

3 (a) H. Xiang, J. Cheng, X. Ma, X. Zhou and J. J. Chruma, *Chem. Soc. Rev.*, 2013, **42**, 6128-6185; (b) F. Anzengruber, P. Avci, L. F. de Freitas and M. R. Hamblin, *Photochem. Photobiol. Sci.*, 2015, **14**, 1492–1509; (c) W. Zhang, X. Sun, T. Huang, X. Pan, P. Sun, J. Li, H. Zhang, X. Lu, Q. Fan and W. Huang, *Chem. Commun.*, 2019, **55**, 9487–9490; (d) Z. Cao, L. Feng, G. Zhang, J. Wang, S. Shen, D. Li and X. Yang, *Biomaterials*, 2018, **155**, 103–111; (e) Q. Wang, Y. Dai, J. Xu, J. Cai, X. Niu, L. Zhang, R. Chen, Q. Shen, W. Huang and Q. Fan, *Adv. Funct. Mater.*, 2019, **29**, 1901480.

4 (a) L. Yuan, W. Y. Lin, S. Zhao, W. S. Gao, B. Chen, L. W. He and S. S. Zhu, *J. Am. Chem. Soc.* 2012, **134**, 13510–13523; (b) J. Zhang, R. Cui, C. Gao, L. Bian, Y. Pu, X. Zhu, X. Li and W. Huang, Small, 2019, **15**, 1904688; (c) Y. Ning, M. Zhu and J.-L. Zhang, *Coord. Chem. Rev.*, 2019, **399**, 213028; (d) N. Toriumi, N. Asano, T. Ikeno, A. Muranaka, K. Hanaoka, Y. Urano and M. Uchiyama, *Angew. Chem Int. Ed.*, 2019, **58**, 7788–7791; (e) R. Mengji, C. Acharya, V. Vangala and A. Jana, *Chem. Commun.*, 2019, **55**, 14182–14185; (f) D. Cheng, J. Peng, Y. Lv, D. Su, D. Liu, M. Chen, L. Yuan and X. Zhang, *J. Am. Chem. Soc.*, 2019, **141**, 6352–6361.

5 (a) A. Zebibula, N. Alifu, L. Xia, C. Sun, X. Yu, D. Xue, L. Liu, G. Li and J. Qian, *Adv. Funct. Mater.*, 2018, **28**, 1703451; (b) P. Zhao, Q. Xu, J. Tao, Z. Jin, Y. Pan, C. Yu and Z. Yu, *Wiley Interdiscip. Rev. Nanomedicine Nanobiotechnology*, 2018, **10**, e1483; (c) P. Jiang, C.-N. Zhu, Z.-L. Zhang, Z.-Q. Tian and D.-W. Pang, *Biomaterials*, 2012, **33**, 5130–5135; (d) J. Zhang, R. Cui, X. Li, X. Liu and W. Huang, *J. Mater. Chem. A*, 2017, **5**, 23536-23542.

6 (a) S. Luo, E. Zhang, Y. Su, T. Cheng and C. Shi, *Biomaterials*, 2011, **32**, 7127–7138; b) L. Yuan, W. Lin, K. Zheng, L. He and W. Huang, *Chem. Soc. Rev.*, 2013, **42**, 622–661; (c) G. Hong, A. L. Antaris and H. Dai, *Nat. Biomed. Eng.*, 2017, **1**, 0010.

7 (a) S. W. Botchway, M. Charnley, J. W. Haycock, A. W. Parker, D. L. Rochester, J. A. Weinstein and J. A. G. Williams, *Proc. Natl. Acad. Sci.*, 2008, **105**, 16071–16076; (b) Y. Fan, J. Zhao, Q. Yan, P. R. Chen and D. Zhao, *ACS Appl. Mater. Interfaces*, 2014, **6**, 3122–3131; (c) Y. Liu, P. Zhang, X. Fang, G. Wu, S. Chen, Z. Zhang, H. Chao, W. Tan and L. Xu, *Dalton Trans.*, 2017, **46**, 4777–4785.

8 C. Wu, H.-F. Chen, K.-T. Wong and M. E. Thompson, *J. Am. Chem. Soc.*, 2010, **132**, 3133–3139.

9 (a) F. Dumur, G. Nasr, G. Wantz, C. R. Mayer, E. Dumas, A. Guerlin, F. Miomandre, G. Clavier, D. Bertin and D. Gigmes, *Org. Electron.*, 2011, **12**, 1683–1694; (b) V. Fiorini, A. D'Ignazio, K. D. M. Magee, M. I. Ogden, M. Massi and S. Stagni, *Dalton Trans.*, 2016, **45**, 3256–3259.

10 S. Guo, T. Huang, S. Liu, K. Y. Zhang, H. Yang, J. Han, Q. Zhao and W. Huang, *Chem. Sci.*, 2017, **8**, 348–360.

11 (a) Y. Ma, H. Liang, Y. Zeng, H. Yang, C.-L. Ho, W. Xu, Q. Zhao, W. Huang and W.-Y. Wong, *Chem. Sci.*, 2016, **7**, 3338–3346. (b) Y. Ma, S. J. Zhang, H. J. Wei, Y. F. Dong, L. Shen, S. J. Liu, Q. Zhao, L. Liu and W.-Y. Wong, *Dalton Trans.*, 2018, **47**, 5582–5588; (c) Y. Ma, Y. F. Dong, L. Zou, L. Shen, S. Y. Liu, S. J. Liu, W. Huang, Q. Zhao and W.-Y. Wong, *Eur. J. Inorg. Chem.* 2018, 2345–2349.

12 M. Mauro, K. C. Schuermann, R. Prétôt, A. Hafner, P. Mercandelli, A. Sironi and L. De Cola, *Angew. Chem. Int. Ed.*, 2010, **49**, 1222–1226.

13 V. C.-H. Wong, C. Po, S. Y.-L. Leung, A. K.-W. Chan, S. Yang, B. Zhu, X. Cui and V. W.-W. Yam, *J. Am. Chem. Soc.*, 2018, **140**, 657–666.

14 (a) H.-L. Au-Yeung, A. Y.-Y. Tam, S. Y.-L. Leung and V. W.-W. Yam, *Chem. Sci.*, 2017, **8**, 2267–2276; (b) B. Ma, P. I. Djurovich, S. Garon, B. Alleyne and M. E. Thompson, *Adv. Funct. Mater.*, 2006, **16**, 2438–2446; (c) Y. Tanaka, K. M. C. Wong and V. W.-W. Yam, *Chem. Sci.*, 2012, **3**, 1185–1191; (d) S. C. F. Kui, S. S.-Y. Chui, C.-M. Che and N. Zhu, *J. Am. Chem. Soc.*, 2006, **128**, 8297–8309; (e) B. Ma, J. Li, P. I. Djurovich, M. Yousufuddin, R. Bau and M. E. Thompson, *J. Am. Chem. Soc.*, 2005, **127**, 28–29; (f) Y. Ma, W. W. Zhao, P. F. She, S. Y. Liu, L. Shen, X. L. Li, S. J. Liu, Q. Zhao, W. Huang and W.-Y. Wong, *Small Methods* 2019, 1900142.

15 (a) A. F. Rausch, U. V. Monkowius, M. Zabel and H. Yersin, *Inorg. Chem.*, 2010, **49**, 7818–7825; (b) J. Forniés, S. Fuertes, J. A. López, A. Martín and V. Sicilia, *Inorg. Chem.*, 2008, **47**, 7166–7176; (c) S. S. Pasha, P. Das, N. P. Rath, D. Bandyopadhyay, N. R. Jana and I. R. Laskar, *Inorg. Chem. Commun.*, 2016, **67**, 107–111.

16 M. E. El-Khouly and S. Fukuzumi, *J. Porphyr. Phthalocyanines*, 2011, **15**, 111–117.

17 (a) S. Luo, E. Zhang, Y. Su, T. Cheng and C. Shi, *Biomaterials*, 2011, **32**, 7127–7138; (b) H. Lu, Y. Zheng, X. Zhao, L. Wang, S. Ma, X. Han, B. Xu, W. Tian and H. Gao, *Angew. Chem. Int. Ed.*, 2016, **55**, 155–159.